# Loading-Rate Dependence of Individual Ligand–Receptor Bond-Rupture Forces Studied by Atomic Force Microscopy

**ARTICLE** *in* LANGMUIR · MAY 2001

Impact Factor: 4.46 · DOI: 10.1021/la001569g



**3 AUTHORS**, INCLUDING:

Ying-Jie Zhu
Chinese Academy of Sciences
**215** PUBLICATIONS **6,969** CITATIONS
SEE PROFILE

Thomas Beebe
University of Delaware
**99** PUBLICATIONS **4,041** CITATIONS
SEE PROFILE

# Loading-Rate Dependence of Individual Ligand−Receptor Bond-Rupture Forces Studied by Atomic Force Microscopy

Yu-Shiu Lo, Ying-Jie Zhu, and Thomas P. Beebe, Jr.*

*Department of Chemistry & Surface Analysis Facility, University of Utah, Salt Lake City, Utah 84112*

*Received November 10, 2000. In Final Form: March 26, 2001*

It is known that bond strength is a dynamic property that is dependent upon the force loading rate applied during the rupturing of a bond. For biotin−avidin and biotin−streptavidin systems, dynamic force spectra, which are plots of bond strength vs $\log_e$(loading rate), have been acquired in a recent biomembrane force probe (BFP) study[1] at force loading rates in the range 0.05−60 000 pN/s. In the present study, the dynamic force spectrum of the biotin−streptavidin bond strength in solution was extended from loading rates of $\sim 10^4$ to $\sim 10^7$ pN/s with the atomic force microscope (AFM). A Poisson statistical analysis method was applied to extract the magnitude of individual bond-rupture forces and nonspecific interactions from the AFM force−distance curve measurements. The bond strengths were found to scale linearly with the logarithm of the loading rate. The nonspecific interactions also exhibited a linear dependence on the logarithm of loading rate, although not increasing as rapidly as the specific interactions. The dynamic force spectra acquired here with the AFM combined well with BFP measurements by Merkel et al. The combined spectrum exhibited two linear regimes, consistent with the view that multiple energy barriers are present along the unbinding coordinate of the biotin−streptavidin complex. This study demonstrated that unbinding forces measured by different techniques are in agreement and can be used together to obtain a dynamic force spectrum covering 9 orders of magnitude in loading rate.

## Introduction

Noncovalent ligand−receptor interactions are critical to life because of their important roles in governing numerous biological events and processes. Direct measurements of weak biochemical interactions at the single-molecule level have been feasible with the advent of various sensitive force-probing techniques, including optical tweezers,[2−4] biomembrane force probe (BFP),[5−8] and atomic force microscopy (AFM).[9−14] In these measurements, an external force is exerted on the molecular complex. Under the application of external force, the strength of molecular binding is governed by kinetic traps.[15] In contrast to equilibrium binding properties, the bond-rupture forces of weak chemical or biochemical bonds are not constants but instead are dependent upon the conditions of the experiments and in particular the rate of force that is applied to the ligand−receptor complex (the "loading rate").

Several studies using molecular dynamics (MD) simulations have been carried out to assist the interpretation of force-probing experiments in terms of potential energy surfaces and to develop insights into the force-induced rupture process.[16−19] Force profiles obtained in these simulations provide insight into the complex mechanisms of biotin−streptavidin rupture. The authors attributed the binding force to a network of hydrogen bonds between the ligand and the walls of the binding pocket.[16] Izrailev et al. and Balsera et al. used MD simulations of a few nanoseconds total duration to reconstruct the essential features of the binding potential of macromolecular complexes.[17,18] Due to the disparity of time scale between simulated rupture processes (picosecond to nanosecond) and the AFM or BFP experiments as well as the natural process (millisecond to second), the simulated unbinding strengths probably cannot readily be extrapolated to the experimentally measured rupture forces. Nevertheless, the simulations are very useful for gaining a qualitative insight into the essential features of the unbinding process.

That the bond-rupture force should depend on the rate at which the bonds are loaded follows from an understanding of the dynamic environment and thermal bath in which the bound complex exists. Impulsive, thermally driven collisions with solvent molecules will occasionally act along the unbinding coordinate to assist the off-rate and dissociate the complex. Although the likelihood of such high-energy impulses decays exponentially with

* Corresponding author. Phone (801) 581-5383, FAX (801) 581-8433, e-mail beebe@chem.utah.edu.

(1) Merkel, R.; Nassoy, P.; Leung, A.; Ritchie, K.; Evans, E. *Nature* **1999**, *397*, 50−53.
(2) Kuo, S. C.; Sheetz, M. P. *Science* **1993**, *260*, 232−234.
(3) Kellermayer, M. S. Z.; Smith, S. B.; Granzier, H. L.; Bustamante, C. *Science* **1997**, *276*, 1112−1116.
(4) Tskhovrebova, L.; Trinick, J.; Sleep, J. A.; Simmons, R. M. *Nature* **1997**, *387*, 308−312.
(5) Evans, E.; Berk, D.; Leung, A. *Biophys. J.* **1991**, *59*, 838−848.
(6) Evans, E.; Berk, D.; Leung, A.; Mohandas, N. *Biophys. J.* **1991**, *59*, 849−860.
(7) Berk, D.; Evans, E. *Biophys. J.* **1991**, *59*, 861−872.
(8) Evans, E.; Ritchie, K.; Merkel, R. *Biophys. J.* **1995**, *68*, 2580−2587.
(9) Binnig, G.; Quate, C. F.; Gerber, C. *Phys. Rev. Lett.* **1986**, *56*, 930−933.
(10) Hoh, J. H.; Cleveland, J. P.; Prater, C. B.; Revel, J.-P.; Hansma, P. K. *J. Am. Chem. Soc.* **1992**, *114*, 4917−4918.
(11) Florin, E.-L.; Moy, V. T.; Gaub, H. E. *Science* **1994**, *264*, 415−417.
(12) Lee, G. U.; Kidwell, D. A.; Colton, R. J. *Langmuir* **1994**, *10*, 354−357.
(13) Dammer, U.; Hegner, M.; Anselmetti, D.; Wagner, P.; Dreier, M.; Huber, W.; Guntherodt, H. J. *Biophys. J.* **1996**, *70*, 2437−2441.
(14) Lo, Y.-S.; Huefner, N. D.; Chan, W. S.; Stevens, F.; Harris, J. M.; Beebe, T. P., Jr. *Langmuir* **1999**, *15*, 1373−1382.
(15) Evans, E.; Ritchie, K. *Biophys. J.* **1997**, *72*, 1541−1555.
(16) Grubmüller, H.; Heymann, B.; Tavan, P. *Science* **1996**, *271*, 997−999.
(17) Izrailev, S.; Stepaniants, S.; Balsera, M.; Oono, Y.; Schulten, K. *Biophys. J.* **1997**, *72*, 1568−1581.
(18) Balsera, M.; Stepaniants, S.; Izrailev, S.; Oono, Y.; Schulten, K. *Biophys. J.* **1997**, *73*, 1281−1287.
(19) Marrink, S.-J.; Berger, O.; Tieleman, P.; Jähnig, F. *Biophys. J.* **1998**, *74*, 931−943.

10.1021/la001569g CCC: $20.00 
Published on Web 05/12/2001

energy, their occurrence increases with time. Thus, at the slowest loading rates one can expect more assistance from fluctuations in the thermal bath, resulting in a lower apparent bond-rupture force. On the other hand, fewer assistive impulses are likely to occur in the relatively shorter time scale of a bond-rupture experiment conducted at high bond-loading rates, resulting in a higher apparent bond-rupture force.

A detailed study of the dynamic nature of bond strengths has been conducted by Evans and Ritchie using extended Kramers' theory and smart Monte Carlo (SMC) simulations.[15] Within the framework of the Bell model,[20] Evans et al. and others[15,21,22] showed that, for a system with a single energy barrier along the unbinding path, the bond strength increased in proportion to the logarithm of the loading rate. This logarithmic dependence originates from the exponential amplification of the off-rate as applied external force rises. This linear regime spanned several orders of magnitude in loading rate. On the basis of the theoretical derivation, increasing loading rate always leads to an increase of measured rupture force, which is referred to as the "Bell–Evans effect".[23]

Measurements of bond-rupture forces as a function of the force loading rate, now known as dynamic force spectroscopy, have been performed in several biological systems using AFM[21–26] and BFP techniques.[1,27] The interactions between biotin–streptavidin (or biotin–avidin) complexes are among the strongest known protein–ligand interactions.[28,29] The bond strengths of biotin–avidin and biotin–streptavidin complexes have been widely investigated,[11,12,14,30–35] including a recent BFP dynamic force spectroscopy study.[1] Merkel et al. showed that the landscapes of the biotin–(strept)avidin systems comprise multiple energy barriers based on the observation of the ascending slope changes in the linear regimes of the dynamic force spectra.[1] This was supported by a recent theoretical study on a constructed model system with multiple energy barriers.[36] Due to the softness of the BFP membrane force transducers, the loading rates that could be probed in the BFP were of a much lower range than the rates that are in general achievable in the AFM. The fastest accessible BFP loading rates ($\sim 10^5$ pN/s) are approximately equal to the slowest practical AFM loading rates. In the BFP work by Merkel et al., the dynamic force spectra of the biotin–avidin and biotin–streptavidin interactions were acquired at loading rates between $10^{-2}$ and $10^5$ pN/s. To extend the range of these spectra, we probed the biotin–streptavidin unbinding forces at loading rates of $10^4$–$10^7$ pN/s with the AFM. The extended section of the force spectrum reported in the present work combined well with the spectrum acquired by Merkel et al. at lower loading rates. This demonstrates that unbinding forces measured by different techniques are in good agreement and together can be used to obtain a dynamic force spectrum covering 9 orders of magnitude in loading rate.

## Experimental Section

**Preparation of Modified Tips and Substrates.** The surface modification with biotin or streptavidin of AFM tips and substrates followed the protocol used in our previous study[14] and that of others.[12,32–34] Glass microscope slides (Fisher Scientific, Pittsburgh, PA) and as-received commercial $Si_3N_4$ AFM cantilever tips (Park Scientific, Sunnyvale, CA) were soaked in a mixture of concentrated $H_2SO_4$ and 30% $H_2O_2$ (70:30 v/v) ("piranha solution") for 30 min.[37] **The piranha solution has a very strong oxidizing power and is extremely dangerous to handle. Goggles, face shields, and gloves are needed for protection.** Glass substrates were then washed five times by ultrasonication in 18 MΩ·cm Milli-Q water (Millipore, Bedford, MA) and dried at 150 °C for 1 h. The AFM cantilever tips were rinsed with copious amounts of 18 MΩ·cm Milli-Q water and dried at 150 °C for 1 h. To create biotin-functionalized tips and surfaces, the cleaned glass substrates and cleaned $Si_3N_4$ AFM cantilever tips were incubated in 1 mg/mL biotinylated bovine serum albumin (BBSA, Sigma, St. Louis, MO) solution in phosphate-buffered saline (PBS; 20 mM $Na_2HPO_4$, 150 mM NaCl, Milli-Q water, pH 7.0) at room temperature overnight. The protein albumin serves as a bearer of biotin on a large-footprint "glue" layer that adsorbs strongly and irreversibly under these conditions. Avidin and streptavidin-functionalized tips and substrates were prepared freshly from biotin-modified surfaces via 30 min incubation in 100 μg/mL avidin or streptavidin (ICN, Costa Mesa, CA) in PBS immediately prior to use. The protein-coated AFM cantilever tips and substrates were characterized by X-ray photoelectron spectroscopy (XPS) and time-of-flight secondary ion mass spectrometry (TOF-SIMS).

**XPS.** XPS analysis was performed using an ESCALab 220i-XL electron spectrometer (VG Scientific, UK) with a monochromatic Al Kα (1486.7 eV) X-ray source. Survey spectra were acquired using a 100 eV pass energy while high-resolution, multiplex spectra of the individual elements were acquired using a 20 eV pass energy and were signal averaged for 50 scans. A low-energy electron flood gun was used to stabilize and compensate for sample charging. Peak positions were assigned by referencing the methylene component of the C 1s peak to a binding energy of 284.6 eV and linearly shifting all other peaks by an equal amount, as is customary.

**TOF-SIMS.** Static TOF-SIMS was performed with a TOF-SIMS instrument (TOF-SIMS IV, ION-TOF, Münster, Germany). Spectra were acquired using a 25 keV monoisotopic $^{69}Ga^+$ primary ion beam generated by a $Ga^+$ ion gun of the same TOF-SIMS instrument. "Bunched mode" was used to achieve highest mass resolution ($m/\Delta m \approx 10\,000$) in the mass spectra. The typical target current of the primary $Ga^+$ beam in the bunched mode was about 3 pA with a prebunched pulse width of 20 ns. The raster area of the $Ga^+$ ion gun was $500 \times 500$ μm². To obtain spatially resolved ion images, $Ga^+$ was used as the primary ion with kinetic energy of 25 keV and a current of 1 pA. The images were obtained with a pulse width of 120 ns, and image sizes are given in the figures. In all cases, charge compensation was achieved by applying low-energy electrons (~20 eV) from a pulsed

(20) Bell, G. I. *Science* **1978**, *200*, 618–627.
(21) Strunz, T.; Oroszlan, K.; Schäfer, R.; Güntherodt, H.-J. *Proc. Natl. Acad. Sci. U.S.A.* **1999**, *96*, 11277–11282.
(22) Schwesinger, F.; Ros, R.; Strunz, T.; Anselmetti, D.; Güntherodt, H.-J.; Honegger, A.; Jermutus, L.; Tiefenauer, L.; Plückthun, A. *Proc. Natl. Acad. Sci. U.S.A.* **2000**, *97*, 9972–9977.
(23) Gergely, C.; Voegel, J.-C.; Schaaf, P.; Senger, B.; Maaloum, M.; Hörber, J. K. H.; Hemmerlé *Proc. Natl. Acad. Sci. U.S.A.* **2000**, *97*, 10802–10807.
(24) Fritz, J.; Katopodis, A. G.; Kolbinger, F.; Anselmetti, D. *Proc. Natl. Acad. Sci. U.S.A.* **1998**, *95*, 12283–12288.
(25) Rief, M.; Gautel, M.; Oesterhelt, F.; Fernandez, J. M.; Gaub, H. E. *Science* **1997**, *276*, 1109–1112.
(26) Rief, M.; Pascual, J.; Saraste, M.; Gaub, H. E. *J. Mol. Biol.* **1999**, *286*, 553–561.
(27) Evans, E. *Faraday Discuss* **1998**, *111*, 1–16.
(28) Chilkoti, A.; Stayton, P. S. *J. Am. Chem. Soc.* **1995**, *117*, 10622–10628.
(29) Weber, P. C.; Ohlendorf, D. H.; Wendoloski, J. J.; Salemme, F. R. *Science* **1989**, *243*, 85–88.
(30) Zhao, S.; Walker, D. S.; Reichert, W. M. *Langmuir* **1993**, *9*, 3166–3173.
(31) Zhao, S.; Reichert, W. M. *Biophys. J.* **1994**, *66*, 305–309.
(32) Moy, V. T.; Florin, E.-L.; Gaub, H. E. *Colloids Surf. A* **1994**, *93*, 343–348.
(33) Moy, V. T.; Florin, E.-L.; Gaub, H. E. *Science* **1994**, *266*, 257–259.
(34) Allen, S.; Davies, J.; Dawkes, A. C.; Davies, M. C.; Edwards, J. C.; Parker, M. C.; Roberts, C. J.; Sefton, J.; Tendler, S. J. B.; Williams, P. M. *FEBS Lett.* **1996**, *390*, 161–164.
(35) Chilkoti, A.; Boland, T.; Ratner, B. D.; Stayton, P. S. *Biophys. J.* **1995**, *69*, 2125–2130.
(36) Strunz, T.; Oroszlan, K.; Schumakovitch, I.; Güntherodt, H.-J.; Hegner, M. *Biophys. J.* **2000**, *79*, 1206–1212.
(37) Lo, Y.-S.; Huefner, N. D.; Chan, W. S.; Dryden, P.; Hagenhoff, B.; Beebe, T. P., Jr. *Langmuir* **1999**, *15*, 6522–6526.

electron flood gun. All primary $Ga^+$ ion fluences were below the threshold $1 \times 10^{13}$ ions $cm^{-2}$ for static SIMS.

**AFM Force Measurements.** A commercial AFM system (Explorer AFM, Topometrix, Santa Clara, CA)[38] with an optical beam deflection detection system was used to obtain force–distance curves. The noise level of this instrument was ±15 pN in these studies.[39] Commercial AFM tips ($Si_3N_4$ Microlevers, Park Scientific, Sunnyvale, CA)[38] were modified as described above. The force constants of the cantilevers were determined from their individually measured resonance frequencies with a series of added masses.[40] The average force constant for the cantilevers employed here was 0.039 ± 0.003 N/m.

**Calibration of the Tip Scan Velocity.** The force-loading rate was determined from the product of the force constant of the AFM cantilever and the scan velocity of the tip. Although the instrument software (TopoMetrix SPMLab v.3.06.06) allowed the nominal scan speed setting to vary from 0.001 to 10 000 μm/s, in this study tip velocities between 1 and ~200 μm/s were employed.[41] It was found in this work that higher velocities were not practically accessible. Through calibrations (see below) and communications with the manufacturer, it was realized that the tip scan speed is limited by the sampling rate in the instrument applied in this study.[42] At a high selected velocity, the program reduces the tip scan rate to allow a minimum of one sample per data point during the force–distance acquisition; i.e., the real scan speed is not as high as it appears in the software.

All force–distance curves were obtained under neutral phosphate-buffered saline medium at room temperature. Four different tip approach/retract velocities were applied, ranging from 1 to ~200 μm/s. Using cantilevers of this force constant, the loading rate was accordingly varied between $4 \times 10^4$ and $8 \times 10^6$ pN/s. For each tip–substrate system, a set of ~50 force–distance curves was recorded at each loading rate. The force curves were collected and processed with a unique statistical method.

**Poisson Statistical Analysis.** A unique statistical method based on Poisson statistics[43] has been developed in our group and described in detail in previously published papers.[14,44–48] It is important to realize that although the Poisson statistical analysis is not a true single-molecule technique (i.e., a few, to a few tens of tip–surface bonds are measured at once), it can be used to extract individual bond-rupture forces. There are no requirements of any preliminary knowledge of the surface energies or tip–surface contact areas, nor is a large number of measurements necessary. The method does not require single-molecule force resolution to resolve single bond-rupture forces and is therefore an attractive tool for use in conjunction with commercial AFM instrumentation.

## Results

**Surface Characterization.** In our previous study of the biotin–avidin systems, the adsorption of the protein "glue", bovine serum albumin (BSA), onto the glass substrates and silicon nitride AFM cantilever tips has proven to be effective.[14] From the previous results of XPS atomic percentage quantification and contact-angle measurements on substrates incubated overnight in BSA solutions at various concentrations, 1 mg/mL BSA concentration was found to be optimal for protein immobilization under our experimental conditions.[14]

TOF-SIMS analysis of the unmodified and BSA-coated control AFM cantilevers is useful as a complementary type of information.[14] In the present work, biotinylated-BSA-modified and avidin-modified glass substrates, as well as AFM cantilevers, were characterized with TOF-SIMS. Because of the moderately low mass percentage of biotin present in BBSA,[49] no unambiguous molecular fragments of biotin were observed on the BBSA-coated cantilever. The immonium ion, $[H_2N{=}CH{-}R]^+$ at $m/z$ = (29 + R), is typically a prominent peak of most amino acids.[50] The TOF-SIMS positive-ion spectra of a BBSA- and an avidin-modified glass substrate are shown in Figure 1. Peaks that are characteristic of some amino acids[50,51] are summarized in Table 1. Several alkyl fragments are also present in the positive-ion spectra. The hydrocarbon fragments are expected from a biological sample such as a random-sequence protein, or they could result from adventitious hydrocarbon contamination. The spectra acquired on the BBSA- and avidin-modified glass surfaces exhibit a slight difference in their fragmentation patterns. The decrease of the silicon and sodium signals on the avidin-coated substrate is another indication of avidin adsorption on the surface which was previously coated with BBSA.

Four spatially resolved TOF-SIMS ion maps of an avidin-modified AFM cantilever are shown in Figure 2. While hydrogen and methyl groups exist in substantial amounts in proteins, they are also found in many common contaminants. As such, the first two images (A and B)

(38) Park Scientific Instruments and TopoMetrix have merged to form ThermoMicroscopes.

(39) The noise level was estimated from the standard deviation of the flat portions of sampled force–distance curves before jump-in during the advancing process and after pull-off during the retracting process. Sources of noise that affect the force sensitivity of the instrument include thermal and mechanical vibrations and intensity fluctuations of the laser used in the optical detection system.

(40) Cleveland, J. P.; Manne, S.; Bocek, D.; Hansma, P. K. *Rev. Sci. Instrum.* **1993**, *64*, 403–405.

(41) At a scan velocity lower than 1 μm/s, it would take seconds to collect a single force–distance curve and a few minutes to obtain a set of multiple force curves. A considerable amount of thermal drift can take place during this time scale. This may be disadvantageous to the application of the Poisson analysis, which requires multiple measurements of one set to be conducted within a fixed contact area. The applicability of the Poisson analysis method at low loading rates will be examined in a future study.

(42) The sampling rate of the TopoMetrix (now ThermoMicroscopes) Explorer AFM used in this study is 100 kHz. When a high scan speed is selected in the program, the instrument software will reduce the tip scan rate to allow for a minimum of one sample per data point during the force–distance acquisition. For instance, if a 1 μm scan range and 500 points are assigned in a force–distance curve, the highest achievable tip scan rate under this setting would be 1 μm/[500 points/($10^5$ points/s)] = 200 μm/s, no matter how high the selected scan speed is. Being able to select very high apparent scan rates is a bug in the software, according to the manufacturer. We believe it is important to point this out so that researchers in the AFM community are aware of this potential problem, especially when carrying out studies at high scan speeds. To calibrate the tip scan velocity, a 100 Hz sine wave was externally input to the A/D channel as a clock to measure the time a tip traveled through various distances. It was confirmed that the number of data points on the curve determined the amount of time the tip scanned through a given distance. The scan velocity was then determined by the ratio of the distance and the travel time. The sine wave served as an accurate time stamp.

(43) Although the distribution is strictly binomial, with a low probability for the occurrence of a given event (i.e., bond formation), it can be approximated by Poisson statistics. A computer modeling study in our group has shown the Poisson model to be robust and generally applicable as long as bond-formation probabilities are low.[48] In biological systems, factors such as steric hindrance and direction of approach can play a significant role in the interactions between biomolecules. Thus, it is a reasonable assumption that the bond-formation probability is low for most biological interactions between a functionalized tip and substrate.

(44) Wenzler, L. A.; Moyes, G. L.; Raiker, G. N.; Hansen, R. L.; Harris, J. M.; Beebe, T. P., Jr. *Langmuir* **1997**, *13*, 3761–3768.

(45) Wenzler, L. A.; Moyes, G. L.; Harris, J. M.; Beebe, T. P., Jr. *Anal. Chem.* **1997**, *69*, 2855–2861.

(46) Williams, J. M.; Taejoon, H.; Beebe, T. P., Jr. *Langmuir* **1996**, *12*, 1291–1295.

(47) Han, T.; Williams, J. M.; Beebe, T. P., Jr. *Anal. Chim. Acta* **1995**, *307*, 365–376.

(48) Stevens, F.; Lo, Y.-S.; Harris, J. M.; Beebe, T. P., Jr. *Langmuir* **1999**, *15*, 207–213.

(49) There are approximately 8–12 mol of biotin ($C_{10}H_{16}N_2O_3S$, MW = 244.3) per mole of bovine serum albumin (MW ≈ 67 kDa) in the BBSA used in this study. The amount of biotin in BBSA is less than 5% in mass, which makes it difficult to probe molecular fragments of biotin by TOF-SIMS, especially amid the complexity of other peaks from protein fragments.

(50) Mantus, D. S.; Ratner, B. D. *Anal. Chem.* **1993**, *65*, 1431–1438.

(51) Lhoest, J.-B.; Castner, D. G. *Proceedings of the 11th Annual SIMS Workshop, Austin, TX*, 1998; pp 41–43.

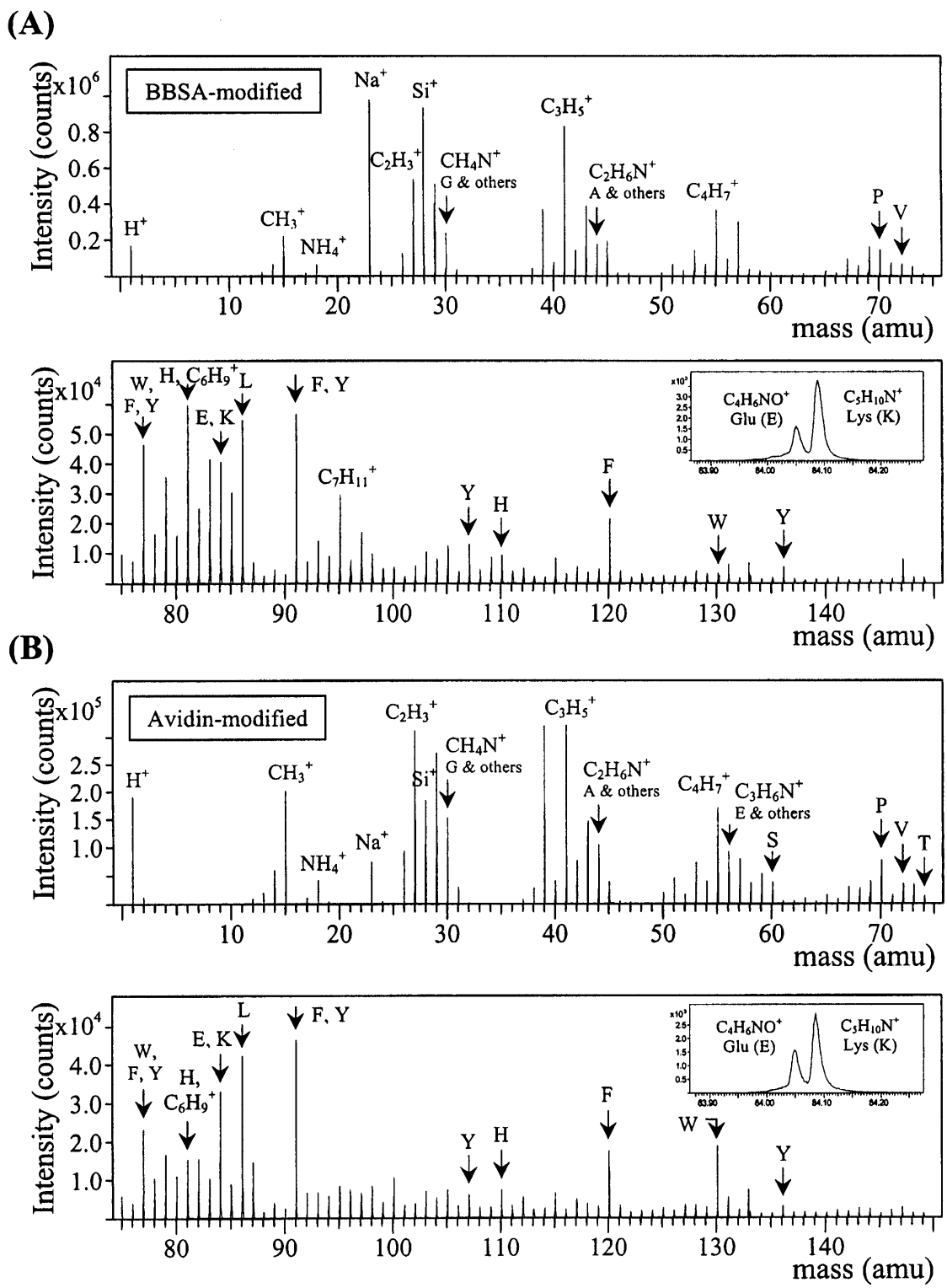


**Figure 1.** TOF-SIMS positive-ion spectra of a BBSA- and an avidin-modified glass substrate. Major peaks are identified. Peaks characteristic of some amino acids are indicated with arrows and labeled with the one-letter abbreviation (see Table 1). The two different protein-coated surfaces exhibit slightly different fragmentation patterns. The decrease of silicon and sodium signals arising from the glass substrate is an indication of the avidin coating on the surface which was previously modified with BBSA.

serve primarily to define the shape and condition of the AFM cantilever. Images C and D depict ion maps of two positive-ion fragments, $CH_4N^+$ and $C_2H_6N^+$, that are characteristic of the amino acids glycine and alanine.[50] These images are indicative of the presence of proteins on the cantilevers as a homogeneous coating (not patchy) on the micron scale.

**Force–Distance Control Experiments.** The schematic of the biotinylated bovine serum albumin (BBSA-) and streptavidin-modified glass substrate and AFM tip (or vice versa) is shown in Figure 3A. In our previous study of the biotin–biotin and BSA–BSA control systems,[14] no noticeable unbinding forces were observed (data not shown), which suggested that the forces measured in the BBSA–streptavidin system were attributed to the specific biotin–streptavidin interaction. This was further supported from the blocking control experiments in which a small amount of free streptavidin was injected between

**Table 1. Summary of Major Peaks of Amino Acids in the TOF-SIMS Positive-Ion Mass Spectra of BBSA- and Avidin-Modified Glass Substrates**

| nominal mass (amu) | ion fragment | exact mass (amu) | characteristic amino acid source |
|---|---|---|---|
| 30 | $CH_4N^+$ | 30.0344 | Gly[a] |
| 44 | $C_2H_6N^+$ | 44.0500 | Ala[a] |
| 56 | $C_3H_6N^+$ | 56.0500 | Glu[a] |
| 60 | $C_2H_6NO^+$ | 60.0449 | Ser |
| 70 | $C_4H_8N^+$ | 70.0657 | Pro |
| 72 | $C_4H_{10}N^+$ | 72.0813 | Val |
| 74 | $C_3H_8NO^+$ | 74.0606 | Thr |
| 77 | $C_6H_5^+$ | 77.0391 | Trp[a] |
| 81 | $C_4H_5N_2^+$ | 81.0453 | His |
| 84 | $C_4H_6NO^+$ | 84.0449 | Glu |
| | $C_5H_{10}N^+$ | 84.0813 | Lys |
| 86 | $C_5H_{12}N^+$ | 86.0970 | Leu |
| 91 | $C_7H_7^+$ | 91.0548 | Phe[a] |
| 107 | $C_7H_7O^+$ | 107.0497 | Tyr |
| 110 | $C_5H_8N_3^+$ | 110.0718 | His |
| 120 | $C_8H_{10}N^+$ | 120.0813 | Phe |
| 130 | $C_9H_8N^+$ | 130.0657 | Trp |
| 136 | $C_8H_{10}NO^+$ | 136.0762 | Tyr |

[a] Although these peaks are characteristic of the amino acids listed in the table, they can also be produced from fragmentation of other amino acids. For example, $CH_4N^+$ at $m/z$ 30 is also a major peak of Lys and a minor peak of several other amino acids.[50]

the BBSA–streptavidin system during force measurements. The free streptavidin molecules apparently blocked the binding sites on the BBSA-modified surface and resulted in the extinction of the adhesive forces detected before the injection.[14]

In some force curves there were multiple steps in the retracting process which may be attributed to multiple or sequential breaking of interacting bonds between the probe and the substrate.[11,13,14,21,52–54] When observed, the adhesive force for each step was measured and treated individually. In Figure 3, examples of a typical (B) force–distance curve and a less common (C) curve with multiple pull-off steps are shown.

**Dynamic Force Spectroscopy.** To study the rate dependence of the ligand–receptor unbinding forces, the tip approach and retract velocity were varied within the range of 1 and ~200 μm/s. The loading rate, which was determined from the product of the cantilever force constant (individually measured) and the tip retract velocity, was between $4 \times 10^4$ and $8 \times 10^6$ pN/s. Six to eight sets of measurements, each composed of 38–87 individual force measurements, were acquired at five different loading rates. Based on the Poisson analysis method, the slope of the linear regression curve in the variance vs mean plot represented the magnitude of the specific, individual bond-rupture force $F_i$. The variance vs mean of eight sets of force measurements taken at the loading rate of $3.7 \times 10^6$ pN/s is plotted in Figure 4. The individual unbinding forces of the biotin–streptavidin interaction determined by the Poisson method at five different loading rates are listed in Table 2. The rupture forces increased with the loading rate. The individual bond-rupture force vs loading rate plot is shown in Figure 5A on a logarithmic scale, as is now customary for dynamic force spectra.

Through application of the Poisson method, the nonspecific interaction, $F_0$, can be determined from the $y$-intercept of the linear regression curve, $-F_iF_0$, in the variance vs mean plot. The nonspecific interactions in the biotin–streptavidin systems under different loading rates, calculated from the ratio of the absolute value of the intercept ($F_iF_0$) and the slope ($F_i$), are summarized in Table 2 and are plotted in Figure 5B. The nonspecific interaction appears to increase linearly and very weakly with the logarithm of the loading rate.

## Discussion

**Combination of Dynamic Force Spectra Acquired with AFM and BFP.** A dynamic force spectroscopy study of biotin–streptavidin bond strength has recently been carried out with the biomembrane force probe by Merkel et al.[1] With a force constant of the BFP membrane transducer in the range 0.1–3 pN/nm, and a retract speed in the range 1–20 000 nm/s, the nominal loading rates applied in the BFP study were between $5 \times 10^{-2}$ and $6 \times 10^4$ pN/s. In the present AFM study, the average force constant of the AFM cantilevers employed was 39 ± 3 pN/nm, 10–40 times stiffer, and the tip retract speed was varied from $1 \times 10^3$ to $2 \times 10^5$ nm/s, resulting in loading rates within the range $4 \times 10^4$–$8 \times 10^6$ pN/s. As shown in Figure 6, the force spectrum acquired with AFM in the present study combined well with that acquired by Merkel et al. using BFP,[1] and two linear regimes were observed in the combined spectrum. The first four points of the AFM study lay well on the line extended from the BFP measurements in the second linear regime within the statistical error. The point of the highest loading rate was located above the line, which possibly indicated the emerging of another inner barrier. More studies at the high loading rates are necessary before the third linear regime can be identified.

On the basis of the Bell model, the off-rate of ligand–receptor dissociation ($k_{off}$) increases exponentially with the increase of an externally applied force $F$ as

$$k_{off}(F) = k_{off}(0) \exp\left(\frac{Fx_\beta}{k_B T}\right) \quad (1)$$

where $k_B T$ is the thermal energy and $x_\beta$ is the distance between the bound and the transition state projected along the direction of applied force.[15,21–23,36] This leads to a logarithmic dependence of the unbinding force ($F_i$) on the loading rate ($r$), which is expressed as[21,22,36]

$$F_i = \frac{k_B T}{x_B} \ln\left(\frac{r x_\beta}{k_{off}(0) k_B T}\right) \quad (2)$$

The dependence of unbinding force $F_i$ upon the logarithm of loading rate in a given linear regime in the force spectrum can be expressed as $F_i \sim f_\beta \ln(\text{loading rate}) + \text{constant}$.[15] The slope $f_\beta$ represents the characteristic force scale for a specific energy barrier that dominates in that region of the unbinding pathway. The characteristic force scale $f_\beta$, as seen in the pre-ln term of eq 2, is defined as

(52) Allen, S.; Chen, X.; Davies, J.; Davies, M. C.; Dawkes, A. C.; Edwards, J. C.; Roberts, C. J.; Sefton, J.; Tendler, S. J. B.; Williams, P. M. *Biochemistry* **1997**, *36*, 7457–7463.

(53) Hinterdorfer, P.; Baumgartner, W.; Gruber, H. J.; Schilcher, K.; Schindler, H. *Proc. Natl. Acad. Sci. U.S.A.* **1996**, *93*, 3477–3481.

(54) The presence of multiple steps in the retracting F/S curve has been observed by us and others in several biological systems and is generally attributed to sequential breaking of interacting bonds. The possibility of contact between the AFM tip and the substrate should be low due to the following reasons: (1) The nature of the interactions between the AFM tip and the substrate (protein–glass) is very different from that of the ligand–receptor interactions. The former is expected to be stronger in magnitude than the latter. Thus, they should be well differentiated in the F/S curves if both are present. (2) In our study, surface modification was done via noncovalent adsorption of a biotinylated "glue" protein BSA. If the tip penetrated through the BBSA layer and contacted the glass substrate, it could result in irreproducible F/S curves in subsequent pull-off events due to desorption or damage to the protein films. None of the above were observed in our systems, so we believe that the multiple pull-offs in our F/S curves were mainly due to the sequential breaking of multiple tip–surface bonds.

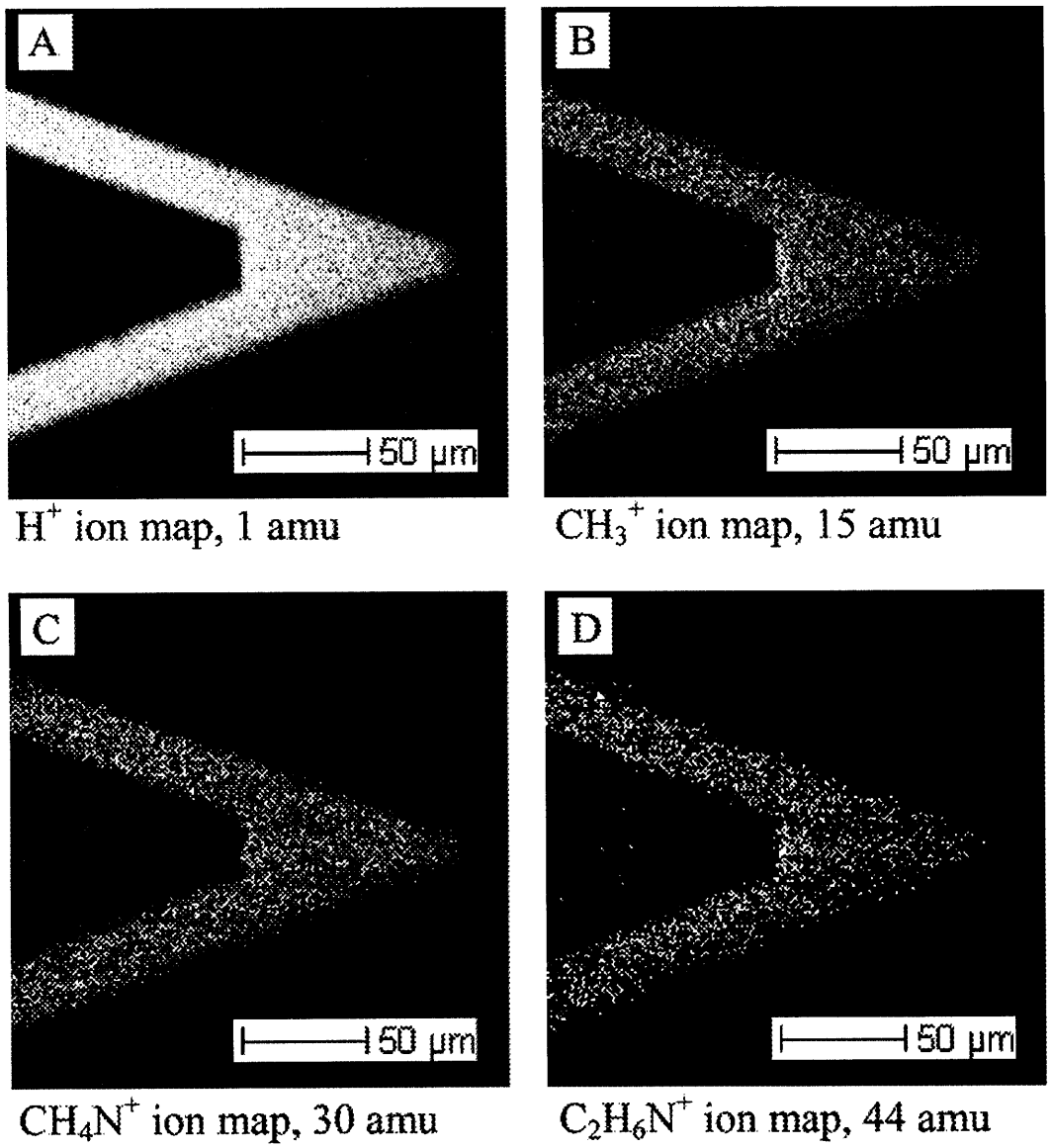


**Figure 2.** Spatially resolved TOF-SIMS ion maps of an avidin-functionalized AFM cantilever. Images A and B depict ion maps of hydrogen and methyl fragment and serve primarily to define the shape and condition of the cantilever. Images C and D depict ion maps of two characteristic positive-ion fragments of amino acids in proteins. These images indicate a homogeneous protein coating on the AFM cantilever on the scale of microns.

**Table 2. Individual Bond-Rupture Force $F_i$ and Nonspecific Interaction $F_0$ between BBSA and Streptavidin in pH 7 Phosphate-Buffered Saline at Various Loading Rates Determined by the Poisson Analysis Method**

| loading rate (pN/s) | $3.90 \times 10^4$ | $3.90 \times 10^5$ | $1.95 \times 10^6$ | $(3.74 \pm 0.31) \times 10^6$ | $(6.28 \pm 1.29) \times 10^6$ |
|---|---|---|---|---|---|
| specific force $F_i$ (from slope, pN) | $167 \pm 20$ | $236 \pm 26$ | $289 \pm 13$ | $350 \pm 30$ | $442 \pm 17$ |
| nonspecific force $F_0$ (from $y$-intercept, pN) | $187 \pm 68$ | $232 \pm 80$ | $244 \pm 23$ | $277 \pm 63$ | $264 \pm 49$ |

the ratio of thermal energy $k_BT$ to the projected bond displacement $x_\beta$ along the reaction coordinate, i.e., $f_\beta = k_BT/x_\beta$.[1,15,55] From the extrapolation to zero unbinding force ($r_{F_i=0}$), the off-rate $k_{off}(0)$ can be determined as[22]

$$k_{off}(0) = \frac{r_{F_i=0}x_\beta}{k_BT} \quad (3)$$

In the recent BFP study,[1] it was demonstrated that the features of the energy landscapes of the biotin–avidin and biotin–streptavidin bonds could be derived from the dynamic force spectra. The continuous sequence of linear regimes with ascending slopes in the dynamic force spectra indicated the presence of multiple energy barriers in the biotin–avidin and biotin–streptavidin complexes.[1,27,36] The slopes of the two linear regimes in Figure 6 were found to be 8 and 34 pN. At room temperature, these corresponded to mapped activation barriers at $x_\beta \approx 5$ and 1.2 Å.[1] An apparent slope change indicated that an outer energy barrier had been overcome and an inner barrier was beginning to govern the kinetics of the unbinding process. The $x$-intercepts (extrapolation to zero force, $r_{F_i=0}$) of the two linear regimes were $\sim 10^{-1}$ and $\sim 10^3$ pN/s. Based on eq 3, they corresponded to the off-rate $k_{off}(0)$ of $\sim 10^{-2}$ and $\sim 30$ s$^{-1}$, respectively.

Unlike the specific unbinding forces of biotin–streptavidin interaction $F_i$, which exhibits more than one regime of linearity, the nonspecific interaction $F_0$ exhibits a single

(55) Evans, E.; Ritchie, K. *Biophys. J.* **1999**, *76*, 2439–2447.

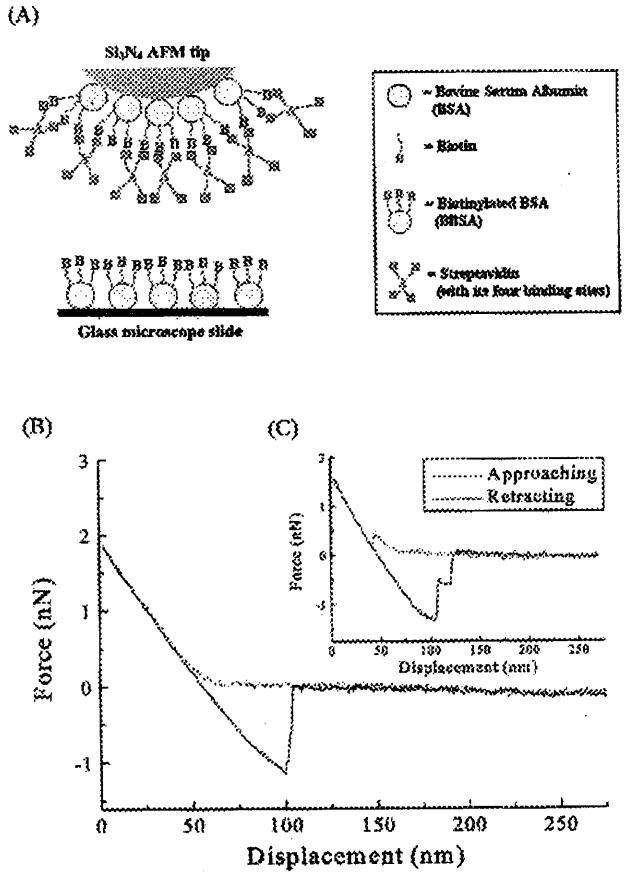


**Figure 3.** AFM measurement of unbinding forces between biotin and streptavidin complexes. (A) Schematic representation of the biotin–streptavidin experimental system. Both the AFM tip and the glass substrate were first functionalized with biotinylated bovine serum ablumin (BBSA). The tip (or vice versa) was further incubated in streptavidin solution to produce a streptavidin-modified tip surface. (B) A typical force–distance curve of the BBSA-streptavidin system. (C) A less typical force–distance curve of the BBSA–streptavidin system with multiple pull-off steps, which may be attributed to multiple or sequential breaking of bonds between the tip and the substrate. Each step was measured and treated individually in the Poisson analysis method.

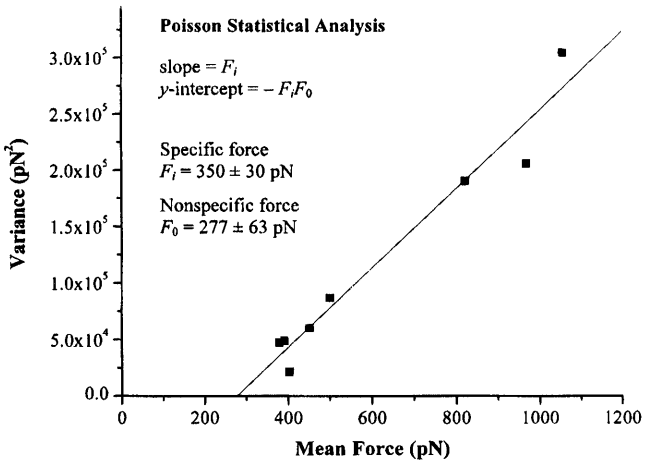


**Figure 4.** Variance vs mean plot of biotin–streptavidin unbinding forces at the loading rate of $3.7 \times 10^6$ pN/s. On the basis of the Poisson analysis method, the slope of the linear regression curve represents the average individual bond-rupture force $F_i$ in the system. The nonspecific force $F_0$ can be estimated from the ratio of the intercept ($-F_iF_0$) and the slope ($F_i$).

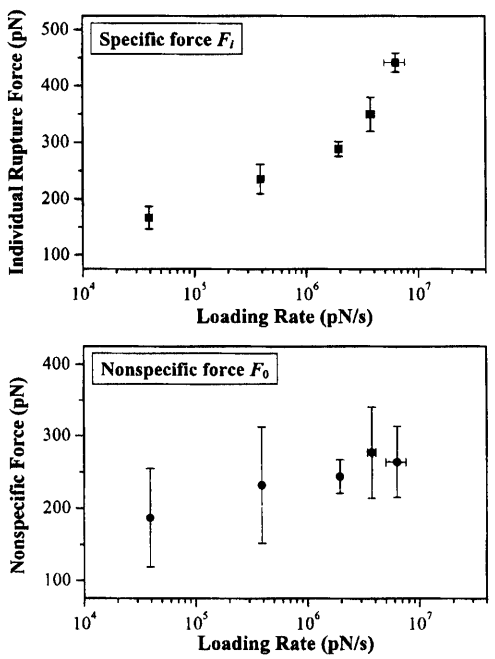


**Figure 5.** Dependence of individual biotin–streptavidin unbinding forces (◆, $F_i$) and nonspecific interactions (●, $F_0$) on AFM loading rate. The individual unbinding forces and nonspecific interactions are determined by the Poisson method from the variance vs mean plots (as shown in Figure 4) and are summarized in Table 2. The error bars correspond to one standard deviation.

slope of ~16 pN in the dynamic force spectrum acquired in this study (Figure 5b), corresponding to a mapped barrier of ~2.6 Å. It seems reasonable that, since the rupture of a specific interaction involves numerous short-range contacts within the binding pocket, there should be multiple energy barriers ("kinetic traps") as the complex moves along this coordinate in phase space. On the other hand, nonspecific interactions are likely to be more long-ranged in nature and are not likely to involve the binding-pocket paradigm, and thus no mountainous features are expected in their energy landscape. We are not aware of any studies, experimental or theoretical, that have attempted to separate and measure specific and nonspecific interactions under the same conditions, let alone as a function of loading rate. We are hopeful that these measurements will stimulate theoretical studies of nonspecific interactions.

**Consideration of Effects from Hydrodynamic Drag and Molecular Linkage.** For force measurements under liquid media, hydrodynamic drag may cause a considerable contribution to the force that is probed, especially at high scan speed. To understand the possible effect of hydrodynamic drag in this study, the deflection of the free-standing AFM cantilever as a function of distance, measured under phosphate-buffered saline, was recorded at various scan velocities in the range of $1 \times 10^3$–$2 \times 10^5$ nm/s. Within this range of scan speed, the signals of the reflected laser beam during both approaching and retracting processes were constant, with slopes close to zero in plots of cantilever deflection vs position (data not shown). This indicated that hydrodynamic drag did not have a significant effect on the cantilever deflection in force measurements obtained at the retract speeds used in this work. The effect of hydrodynamic drag on the molecular species themselves was not addressed in this study and would require a detailed theoretical treatment.

Evans and Ritchie have pointed out that the strengths of weak bonds under dynamic force loading can also be

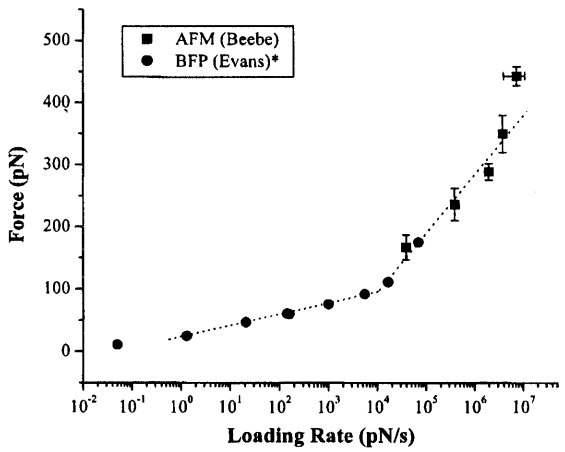


**Figure 6.** Combination of dynamic force spectra for biotin–streptavidin bonds reported in the present AFM study and the previous BFP study (taken from Merkel et al., 1999). The general trend and linear dependence of bond strength on the logarithm of loading rate are illustrated. The data acquired by these two techniques are in agreement and can be combined together to obtain a dynamic force spectrum covering 9 orders of magnitude in loading rate. Error bars were not reported in the work by Merkel et al. (filled circles).

affected by "soft molecular linkages" when the bonds are connected to the probe or the substrate by flexible polymers.[55] Instead of simply considering the stiffness of the force transducer, the total compliance attributed to both the force transducer and the molecular linkage has to be considered to accurately determine the actual force loading experienced by the bonds. The nominal loading rate in the absence of this consideration will be an upper limit on the actual loading rate. Unlike for long polymer linkages such as titin, whose extension has been studied experimentally by AFM[25] and optical tweezers[3,4] and investigated in theoretical work by Evans and Ritchie,[55] the molecular "linkages" used in this AFM study were bovine serum albumin (BSA) proteins. Bovine serum albumin (MW ≈ 67 kDa) is a globular protein with three domains and a repeating double-loop structure formed by paired disulfide bonds between adjacent cysteine residues.[56] These inter- and intrachain covalent disulfide bonds render structural stability to the protein.[56] Although it would be unlikely under these conditions, no sawtooth pattern, as seen in the titin system,[25] was observed in our force–distance curves, indicating that BSA did not denature into a linear peptide sequence. BSA proteins adhere well to silica surfaces, undergoing a structural change upon adsorption.[57–59] Although it is reported that BSA is relatively soft among some other globular proteins,[57–60] once adsorbed onto glass substrates, BSA molecules should be fairly rigid under the force level applied in the AFM measurements. We made the assumption that the total compliance within the cantilever–BBSA–streptavidin system was given by $(k_f + k_L)/k_f k_L$ for "springs" operating in series, where $k_f$ and $k_L$ are force constants of the AFM cantilever and BSA linker, respectively. Under constant compliance, the bond strength would be lowered by $f_\beta \log_e[(k_f + k_L)/k_L]$ at any given apparent loading rate defined by the force constant of the force transducer and the retract speed of the tip.[55] With the assumption that BSAs are compact, "rigid" proteins (i.e., $k_f \ll k_L$), the factor $\log_e[(k_f + k_L)/k_L]$ would be small.[61] Because $k_L$ for BSA is not known, no quantitative information on the effect of molecular linkages can be provided.

## Conclusions

In this AFM study the dynamic force spectrum of biotin–streptavidin bond strength at loading rates ranging from $4 \times 10^4$ to $8 \times 10^6$ pN/s was reported. The Poisson statistical analysis method applied in this study was found to be an effective method to study the individual bond-rupture force. Consistent with the previous BFP study by Evans, the dynamic force spectrum acquired in this work exhibited a linear relationship between the unbinding force and the logarithm of the loading rate. Combining measurements from BFP and AFM, there were two linear regimes in the dynamic force spectrum of the biotin–streptavidin system, indicating that multiple energy barriers are present along the unbinding coordinate. For the first time, nonspecific forces were measured and compared to specific forces. They exhibited a weaker dependence on loading rate.

**Acknowledgment.** We thank Evan Evans for stimulating this study and Vladimir Hlady for advice and discussions. This work was supported by the National Science Foundation (CHE-9357188; DMR-9724307; CHE-9814477), the Alfred P. Sloan Foundation, and the Center for Biopolymers at Interfaces (CBI) at the University of Utah.

LA001569G

(56) Peters, T., Jr.; Reed, R. G. In *Transport by Proteins*; Blauer, G., Sund, H., Eds.; Walter de Gruyter & Co.: New York, 1978.

(57) Kondo, A.; Oku, S.; Higashitani, K. *J. Colloid Interface Sci.* **1991**, *143*, 214–221.

(58) Norde, W.; Favier, J. P. *Colloids Surf.* **1992**, *64*, 87–93.

(59) Sagvolden, G. *Biophys. J.* **1999**, *77*, 526–532.

(60) Tripp, B. C.; Magda, J. J.; Andrade, J. D. *J. Colloid Interface Sci.* **1995**, *173*, 16–27.

(61) Under constant compliance, the bond strength would be lowered by the amount $f_\beta \log_e[(k_f + k_L)/k_L]$ at any given apparent loading rate. To estimate how the elasticity of the molecular linker (BSA in this study) affects bond strength in the dynamic force spectrum, let $g = \log_e[(k_f + k_L)/k_L]$. For $k_f \approx 10k_L$ ("soft BSA"), $g \cong 2.40$. For $k_f \approx k_L$, $g \cong 0.69$. For $10k_f \approx k_L$ ("rigid BSA"), $g \cong 0.1$.